Energy Proceedings
Vol 27, 2022
ISSN 2004-2965

The Catalytic Effect of Iron Oxide Phases on the Conversion of Cellulose-Derived Chars#

Christin Pflieger[1], Till Eckhard[1], Jannik Böttger[1], Jonas Schulwitz[1], Stefan Schmidt[1], Soma Salamon[2], Joachim Landers[2], Heiko Wende[2], Martin Muhler[1], Francesca Cerciello[1*]

1 Lehrstuhl für Technische Chemie, Ruhr-Universität Bochum, Universitätsstr. 150, 44801 Bochum, Germany

2 Fakultät für Physik und Center for Nanointegration Duisburg Essen (CENIDE), Universität Duisburg-Essen, Lotharstr. 1, 47057 Duisburg, Germany

ABSTRACT

Biomass char conversion is substantially influenced by metals contained in the material. One of the main catalytically active metals in biomass is Fe which occurs in various mineral forms. For an implementation of catalytic effects into char conversion models, investigations on mineral type and loading are required. In this work, the catalytic effect of an Fe loading series on the oxidation of an inherently mineral-free char was analysed. Characterisations focused on the Fe phase present in the char identifying its transition from $FeSO_4$ to γ-Fe_2O_3 during doping, and further to ε-Fe_2O_3 and α-Fe_2O_3 upon char oxidation. A very high loading-dependent activity of ε-Fe_2O_3 was found.

Keywords: biomass-derived char, char conversion, Fe minerals, catalytic activity, phase transitions

NOMENCLATURE

Abbreviations	
DTG	Differential thermogravimetric
TPO	Temperature-programmed oxidation
XRD	X-ray diffraction
Symbols	
c	Phase contribution
d_P	Particle diameter
w	Loading

1. INTRODUCTION

For the reduction of global greenhouse gas emissions, a special focus lies on the combustion of biomass-derived fuels.[1] In the combustion process, char conversion is the rate-determining step,[2] which may be strongly influenced by the mineral content of the biomass.[3] Current char conversion models do not account for mineral effects and need to be extended for an accurate prediction of the process.[4] Hence, the assessment of catalytic effects specific for different types and amounts of minerals typically contained in natural biomass is required. In the case of Fe, one of the major catalytically active metals, different minerals were found in biomass and phase transformation was reported to occur during the combustion process.[5] For example, sulfates as primary Fe minerals are transformed into different stable oxides. For these species of the general composition Fe_xO_y, not only different Fe oxidation states, but also different polymorphs of the same oxidation state need to be considered. Most prominently, Fe_2O_3 was found to undergo purely structural phase transitions upon particle agglomeration, from metastable γ-Fe_2O_3 over ε-Fe_2O_3 to the highly stable α-Fe_2O_3.[6]

Aiming at the catalytic effect of Fe on char conversion, an inherently mineral-free char was doped with a loading series of Fe in this work. The reactivity of the samples was investigated by temperature-programmed oxidation (TPO) measurements. Changes in char reactivity were related not only to the amount but also to the type of mineral phase present in the material, thereby establishing structure-activity correlations.

2. MATERIALS AND METHODS

2.1 Synthesis

In a first step, a mineral-free model char was synthesized by hydrothermal carbonisation of microcrystalline cellulose at 200 °C for 24 h and subsequent low heating rate pyrolysis at 800 °C for 2 h.[7] The obtained MH800 char was then selectively doped with $FeSO_4 \cdot 7\,H_2O$ by wet impregnation[8], thereby loading 0.15 – 2.4 wt%. The synthesis was finalised by drying at 105 °C in air and the samples were labelled using their loading w as 'w Fe-MH800'. For example, the sample loaded with 0.15 wt% Fe was labelled as '0.15 Fe-MH800'.

2.2 *Temperature-Programmed Measurements*

TPO measurements were performed by heating about 30 mg of sample with 5 °C min^{-1} in 20% O_2/He using a magnetic suspension balance.[8] Measurement analysis relied on the differential thermo-gravimetric (DTG) curve.

2.3 *Mineral Characterisation*

Mössbauer spectroscopy was performed in transmission geometry using a ^{57}Co(Rh) radiation source mounted on a driving unit operating in constant acceleration mode. The isomer shifts of spectra derived from about 210 - 230 mg of sample material were referenced against α-Fe at room temperature.

Powder X-ray diffraction (XRD) patterns were recorded using a diffractometer (Bruker Discover D8) equipped with θ - θ geometry, Lynxeye-1D detector, and Cu Kα radiation (0.15406 nm, 40 kV, 40 mA). The recording was performed in a 2θ range from 5 - 80 ° with 0.02 ° s^{-1} and data were evaluated using the software DIFFRAC.SUITE EVA with access to the International Centre for Diffraction Data database. Particle diameters were analysed according to the Scherrer equation[9] and Rietveld refinement was performed using the interface Profex 5.0.0[10] with the backend BGMN[11]. The implemented database was extended using structural information from 'The Materials Project'[12].

3. RESULTS AND DISCUSSION

3.1 *TPO Analysis*

The DTG curves derived from the TPO measurements of the Fe loading series are shown in Fig. 1.

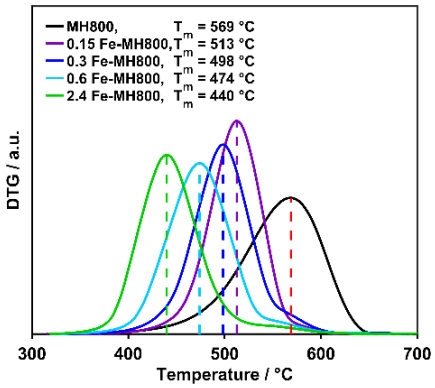

Figure 1. DTG curves of the Fe loading series TPO measurements with marked peak maxima.

The analysis reveals a strong temperature shift of the peak maxima with increasing loading and hence a loading-dependent catalytic effect. Compared with the undoped model char, the temperature of maximum oxidation rate is lowered by up to 129 °C. In addition to these remarkable peak temperatures, a slightly altered peak shape was found. In the high-temperature region of the conversion peaks an additional shoulder was observed especially for the higher loadings of Fe (red dashed line in Fig. 1). The overall shape points towards catalytic char conversion related to the main low-temperature peak and non-catalytic char conversion related to the high-temperature shoulder as there is no significant temperature shift relative to the undoped char for this part.

There are two possible explanations for the observed non-catalytic char conversion. On the one hand, it may be possible that the loading of Fe is too low to affect the entire carbon material, so that there are carbon sites without contact to Fe which are therefore converted according to the non-catalytic pathway. On the other hand, there may be two different Fe mineral phases present during conversion, either simultaneously as a mixture or by transformation due to the temperature increase. Consequently, the (initially) active phase would cause the catalytic conversion of char, whereas final conversion proceeds non-catalytically as there is only a comparatively inactive Fe phase present on the char, which may have been present from the beginning or resulted from phase transition. In case of the first alternative of a too low Fe loading, a decreasing contribution of non-catalytic conversion would be expected for higher Fe loadings, as an increased occurrence of Fe would minimise the possibility of carbon sites being unaffected by Fe. As no such correlation is shown in the curves, the presence of two distinguishable contributions to conversion is assumed to originate from two different present mineral phases of different catalytic activity.

Consequently, oxidation of the Fe-doped chars proceeds predominantly catalysed by a highly active Fe phase, exhibiting a loading dependence of catalytic activity and resulting in a shift of the main peak in the DTG curve towards lower temperatures upon an increased loading. In contrast, the additional contribution of an essentially inactive Fe phase leads to the high-temperature shoulder, which is for all loadings observed in the same temperature range of the undoped char. Future studies including a kinetic modelling of the obtained DTG curves will enable to quantify the extent of the two different catalytic activities as well as the strength of loading-dependence.

3.2 Fe Phase Analysis

To validate the assumption of different Fe phases present during char conversion, characterisation measurements were performed after different treatments of the loaded chars.

3.2.1 As-Synthesised Char

The phase analysis of the as-synthesised char was performed using 2.4 Fe-MH800, as this highest loading was the most promising to achieve phase identification despite the dominating char material. The Mössbauer spectrum obtained with this sample at room temperature is shown in Fig. 2.

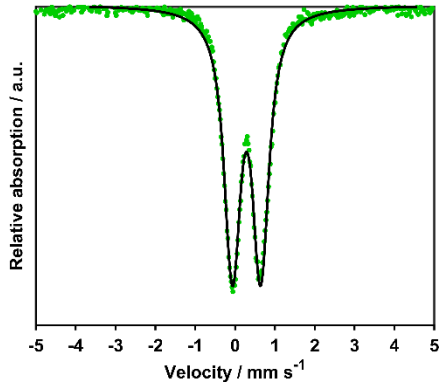

Figure 2. Fitted Mössbauer spectrum obtained with 2.4 Fe-MH800 at room temperature.

The recorded doublet with an isomeric shift of 0.40 mm s^{-1} is characteristic for Fe^{3+}.[13] Consequently, the synthesis procedure led to an oxidised Fe mineral despite the doping with $FeSO_4$. The carbon material significantly lowered the decomposition temperature of $FeSO_4$, as heating of the doped sample was only performed up to a maximum temperature of 105 °C, which is significantly below the decomposition temperature of pure $FeSO_4$ (> 500 °C).[14] A similar decrease of the $FeSO_4$ decomposition temperature due to a surrounding organic matrix has already been observed for lignite and bamboo, but to a lower extent than for the char material in this work.[15, 16] For further analysis of the oxidised phase, XRD measurements were performed. While for the as-synthesised 2.4 Fe-MH800 the particles were too small to obtain mineral-related reflexes and the broad carbon signals were dominating, the XRD pattern of the same loading obtained after isothermal heating to 480 °C in He (Fig. 3) was indicative of either γ-Fe_2O_3 or Fe_3O_4 particles. These phases are undistinguishable by XRD as both oxide species crystallise in the same space group and feature similar lattice parameters.[17]

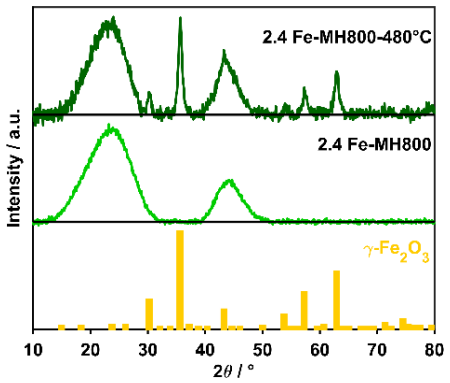

Figure 3. XRD patterns of 2.4 Fe-MH800 as-synthesised and after 3 h of isothermal treatment in He.

However, in combination with the Mössbauer results revealing Fe^{3+}, the identification of γ-Fe_2O_3 as the phase present after the synthesis procedure is achieved, presumably displaying a doublet structure due to superparamagnetic relaxation. Further, an evaluation of the XRD pattern of the heat-treated char revealed an iron-particle diameter of 12 nm. A comparison to the pattern of the as-synthesised char shows that a significant increase of particle size was induced by the thermal treatment, resulting in an increased mineral crystallinity and hence identifiable reflexes. Considering this substantial thermally induced sintering,[18] the particle diameter of γ-Fe_2O_3 after synthesis is known to be far below 12 nm.

3.2.2 *Ash Samples*

Phase transformation by oxidation was investigated by exposing the doped chars to an oxidising treatment at 480 °C, resulting in a complete conversion of the carbon material. For the corresponding ash samples, XRD (Fig. 4) revealed that ε-Fe_2O_3 and α-Fe_2O_3 remained after oxidation, i.e. that further phase transformation of γ-Fe_2O_3 occurred upon char conversion.

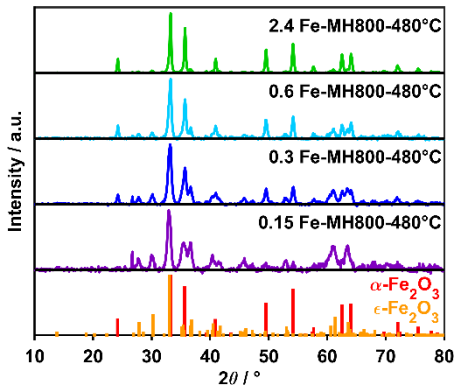

Figure 4. XRD patterns of differently loaded Fe-MH800 samples after isothermal conversion for 3 h in 20% O_2/He.

As oxidation was performed at the same temperature of the purely thermal treatment in Section 3.2.1, the observed phase transition cannot be solely related to thermally induced particle sintering. Instead, a decisive contribution of the oxidative atmosphere and the loss of char is likely. For further analysis, a quantification of the individual phase contributions by a Rietveld refinement of the XRD patterns of the ash samples was performed. The results are summarised in Table 1 along with the particle diameters.

Table 1. Phase contributions c and particle diameters d_P of the ash samples remaining after oxidation of differently loaded Fe-MH800 for 3 h at 480 °C.

Loading	α-Fe_2O_3		ε-Fe_2O_3	
/ wt%	c / -	d_P / nm	c / -	d_P / nm
0.15	0.03	-	0.97	12
0.3	0.20	19	0.80	12
0.6	0.30	25	0.70	15
2.4	0.62	31	0.38	17

The loading dependence of both phase composition and particle size is clearly shown. While for the lowest loading ε-Fe_2O_3 was predominant during oxidation and the concurrent loss of the carbon matrix, oxidation of the intermediate loadings was associated with an increased transition to α-Fe_2O_3. For the highest loading, α-Fe_2O_3 was even the main fraction present after oxidation. Simultaneously, the particles of both phases were found to increase in size with increasing loading. The particle diameter of the minerals during the phase transition from ε-Fe_2O_3 to α-Fe_2O_3 is found to be in the range of 17 – 19 nm. However, for the previous transition of γ-Fe_2O_3 to ε-Fe_2O_3 no size range of transition can be stated as for both phases particles of 12 nm diameter were found. Therefore, this structural transition is indicated to be induced by exposing the material to an oxidative atmosphere.

Following the phase analysis, ε-Fe_2O_3 is identified to be the active phase upon char oxidation for Fe loadings of 0.15 - 0.6 wt%, while for increased conversion degrees in TPO measurements also α-Fe_2O_3 needs to be considered. However, the correlation to particle size indicates that the loss of the surrounding char matrix may contribute significantly to the transition from ε-Fe_2O_3 to α-Fe_2O_3. Hence, the actual phase contribution of α-Fe_2O_3 during oxidation may be lower than its contribution detected in the ash. For a more precise determination of phase contributions during oxidation, an analogous quantification of the different polymorphs in an oxidising atmosphere prior to significant loss of char will be obtained in further studies.

Nevertheless, the phase analysis in this work identified ε-Fe_2O_3 and α-Fe_2O_3 as the Fe phases decisive for char oxidation with a clear loading dependence of their relative abundance and relevance. The mainly present Fe mineral is the highly active ε-Fe_2O_3 phase forming small particles, while increased loadings enhance particle agglomeration and hence the transition to the larger α-Fe_2O_3 particles, contributing to a much lower extent to catalytic char conversion.

4. CONCLUSIONS

The catalytic effect of an Fe loading series on the oxidation of a biomass-derived model char was investigated. The inherently mineral-free char was selectively doped using $FeSO_4$ and reactivities were derived from TPO measurements. Two differently reactive contributions to char conversion were evident and related to the presence of different Fe mineral phases. The corresponding phase analysis after different char treatments revealed the following order of mineral transitions:

$FeSO_4 \rightarrow$ γ-$Fe_2O_3 \rightarrow$ ε-$Fe_2O_3 \rightarrow$ α-Fe_2O_3

Drying at 105 °C in air during synthesis was sufficient to oxidise $FeSO_4$ impregnated onto the char to the metastable γ-Fe_2O_3 present in the as-synthesized char and the char thermally treated at 480 °C in He. Exposure to an oxidising atmosphere of 20% O_2/He at 480 °C induced a further transition to ε-Fe_2O_3, which was the main phase present during char oxidation exhibiting a high loading-dependent catalytic activity. Compared with the undoped model char, the presence of this phase lowered the temperature of maximum oxidation rate in the TPO measurements by up to 129 °C. While for the lowest loading of 0.15 wt% Fe, ε-Fe_2O_3 was the predominant phase throughout conversion, a further transition occurred to α-Fe_2O_3 with larger particles for increased loadings and increased char conversion. This phase contributed with 20% and 30% to the ash of 0.3 Fe-MH800 and 0.6 Fe-MH800, respectively, and was the main phase present after oxidation of 2.4 Fe-MH800 with a contribution of 62%. However, α-Fe_2O_3 exhibited no significant catalytic activity and a negligible contribution to catalytic char oxidation.

ACKNOWLEDGEMENT

Funded by the Deutsche Forschungsgemeinschaft (DFG, German Research Foundation) –Project-ID 215035359– CRC/TRR 129 Oxyflame. ”Gefördert durch die Deutsche Forschungsgemeinschaft (DFG) – Projektnummer 215035359– CRC/TRR 129 Oxyflame”.

Funded by the Deutsche Forschungsgemeinschaft (DFG, German Research Foundation) – Project-ID 388390466– CRC/TRR 247. ”Gefördert durch die Deutsche Forschungsgemeinschaft (DFG) – Projektnummer 388390466– CRC/TRR 247”.

REFERENCES

[1] Roncancio R, Gore JP. CO_2 char gasification: A systematic review from 2014 to 2020. Energy Conversion and Management: X 2021;10:100060.

[2] Du Y, Wang C, Xin H, Che D, Mathews JP. Atomistic Simulation of Coal Char Oxy-Fuel Combustion: Quantifying the Influences of CO_2 to Char Reactivity. Energy Fuels 2019;33(10):10228–36.

[3] Duman G, Uddin MA, Yanik J. The effect of char properties on gasification reactivity. Fuel Processing Technology 2014;118:75–81.

[4] Branca C, Di Blasi C. Burning Dynamics of Straw Chars under the Conditions of Thermal Analysis. Energy Fuels 2021;35(15):12187–99.

[5] Vassilev SV, Baxter D, Vassileva CG. An overview of the behaviour of biomass during combustion: Part I. Phase-mineral transformations of organic and inorganic matter. Fuel 2013;112:391–449.

[6] Sakurai S, Namai A, Hashimoto K, Ohkoshi S-I. First observation of phase transformation of all four Fe_2O_3 phases (gamma -- epsilon -- beta -- alpha-phase). Journal of the American Chemical Society 2009;131(51):18299–303.

[7] Pflieger C, Lotz K, Hilse N, Berger CM, Schiemann M, Debiagi P et al. Catalytic influence of mineral compounds on the reactivity of cellulose-derived char in O_2-, CO_2-, and H_2O-containing atmospheres. Fuel 2021;287:119584.

[8] Eckhard T, Pflieger C, Schmidt S, Böttger J, Senneca O, Schiemann M et al. Catalytic Effects for Cellulose-Based Model Fuels Under Low and High Heating Rate in Air and Oxy-Fuel Atmosphere. SSRN Journal 2022.

[9] Ali K, Sarfraz AK, Mirza IM, Bahadur A, Iqbal S, ul Haq A. Preparation of superparamagnetic maghemite (γ-Fe_2O_3) nanoparticles by wet chemical route and investigation of their magnetic and dielectric properties. Current Applied Physics 2015;15(8):925-9.

[10] Doebelin N, Kleeberg R. Profex: a graphical user interface for the Rietveld refinement program BGMN. J Appl Crystallogr 2015;48(Pt 5):1573–80.

[11] Bergmann J, Friedel P, Kleeberg R. BGMN — a new fundamental parameters based Rietveld program for laboratory X-ray sources, it's use in quantitative analysis and structure investigations. In: CPD Newsletter 1998;20.

[12] Jain A, Ong SP, Hautier G, Chen W, Richards WD, Dacek S et al. Commentary: The Materials Project: A materials genome approach to accelerating materials innovation. APL Materials 2013;1(1):11002.

[13] Devi L, Craje M, Thüne P, Ptasinski KJ, Janssen FJ. Olivine as tar removal catalyst for biomass gasifiers: Catalyst characterization. Applied Catalysis A: General 2005;294(1):68–79.

[14] Masset P, Poinso JY, Poignet JC. TG/DTA/MS Study of the thermal decomposition of $FeSO_4 \cdot 6H_2O$. J Therm Anal Calorim 2006;83(2):457–62.

[15] Zhang D, Yani S. Sulphur transformation during pyrolysis of an Australian lignite. Proceedings of the Combustion Institute 2011;33(2):1747–53.

[16] Pace B, Munroe P, Marjo CE, Thomas P, Gong B, Shepherd J et al. The mechanisms and consequences of inorganic reactions during the production of ferrous sulphate enriched bamboo biochars. Journal of Analytical and Applied Pyrolysis 2018;131:101-12.

[17] Katikaneani P, Vaddepally AK, Reddy Tippana N, Banavath R, Kommu S. Phase Transformation of Iron Oxide Nanoparticles from Hematite to Maghemite in Presence of Polyethylene Glycol: Application as Corrosion Resistant Nanoparticle Paints. Journal of Nanoscience 2016;2016:1–6.

[18] Kramer CM, German R. M. Low-Temperature Sintering of Iron Oxides. J American Ceramic Society 2006;61(7-8):340–2.